



Crack propagation in a Tantalum nano-slab

ALEJANDRO STRACHAN*, TAHIR ÇAĞIN and WILLIAM A. GODDARD III

Materials and Process Simulation Center, Beckman Institute (139-74), California Institute of Technology, Pasadena, CA 91125, U.S.A.

Received 10 March 2001; Accepted in revised form 7 September 2001

Abstract. Using molecular dynamics with an accurate many-body potential for metallic Tantalum, we studied crack propagation in a pre-notched nano-slab under uniaxial strain in a [100] direction. We study dislocation emission from the crack tip for various strain rate and temperatures, focusing on the influence of the local temperature at the crack tip on the propagation of the crack. We find a close connection between the local temperature at the crack tip and dislocation emission.

Keywords: Crack propagation, Ductile fracture, Failure, Molecular dynamics, Tantalum

1. Introduction

Understanding crack propagation and failure is one of the problems facing materials science with mayor technological importance. A complete understanding of the atomistic processes involved in crack propagation is still lacking despite the great efforts done in this field during the last decades.

Molecular Dynamics (MD) simulations using realistic interatomic potentials can provide important insight and a detailed understanding of the several atomistic processes involved in failure. MD has been used in several studies of crack propagation in fcc [1–7] and bcc [8, 9] metals as well in several non metallic systems such as silicon, see for example [10]. Atomistic simulations allow one to study temperature and strain rate effects on crack propagation, brittle to ductile transition, details of the dislocation emission for the crack tip. They also provide a natural link between the atomistic interactions and continuum modeling of failure, leading to the possibility of simulating macroscopic systems for long times to study processes such as failure under cyclic loading or fatigue. The mayor limitations of MD simulations of crack propagation are the short time scales (nanoseconds) and small length scales (millions of atoms). Short time scales lead to high strain rates and small length scales cause dislocation pile-ups and reflection of the sound waves emitted by the crack in cell boundaries. Combined atomistic and continuum modeling is a promising avenue and has been used to study crack propagation [11].

We use an Embedded Atom Model many-body potential for Ta (named qEAM) based on ab initio quantum mechanical (QM) calculations [12, 13]. The qEAM potential correctly reproduces QM data of zero temperature Equation of State for bcc, fcc, and A15 phases of Ta, elastic constants, vacancy formation energy and energetics of a shear transformation in the twinning direction [12]. We have previously used the qEAM with MD to study a variety

*To whom correspondence should be addressed.

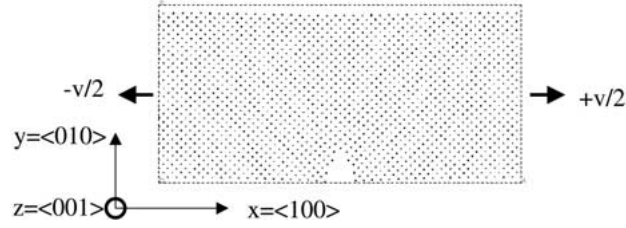


Figure 1. Initial configuration for crack propagation simulations. The simulation cell sizes are $135.81 \text{ \AA} \times 66.57 \text{ \AA} \times 29.95 \text{ \AA}$ and it contains 14328 atoms.

of materials properties such as melting temperature as a function of pressure, dislocation properties, and spall failure [14].

In this paper we study mode I crack propagation in a Ta nano-slab. We use the uniaxial expanding boundary conditions technique [1] to simulate the region near the crack tip of a sample under uniaxial load. We performed simulations for various strain rates and temperatures $T = 300 \text{ K}$ and $T = 600 \text{ K}$. We study the influence of the local temperature of the crack tip on dislocation emission.

The paper is organized as follows. In Section 2 we explain the MD simulations performed to study mode I crack propagation. Section 3 shows our results regarding strain rate and temperature influence on crack propagation in nano slabs. Finally, in Section 4 we present a discussion of our results.

2. MD simulations of mode I crack propagation

The initial configurations for our crack propagation simulations consists of a pre-notched slab, shown in Fig. 1. We build a simulation cell containing $N = 14400$ atoms by replicating the bcc 2-atom unit cell 40 times in the $x = \langle 100 \rangle$ direction, 20 in $y = \langle 010 \rangle$ and 9 in the $z = \langle 001 \rangle$; this leads to a cell with lengths $135.81 \text{ \AA} \times 66.5735 \text{ \AA} \times 29.958 \text{ \AA}$, using the zero pressure lattice parameter at $T = 300 \text{ K}$. Eight rows of atoms along the z direction are removed in order to build the initial notch; we are thus left with $N = 14328$ atoms, see Fig. 1. We impose free boundary conditions in the direction of crack propagation (y direction) and periodic boundary conditions in the x and z directions. The initial configuration for the crack propagation simulations is obtained by straining the system by 2% in the x direction and performing a thermalization using constant temperature and volume (TVN) MD.

In order to simulate mode I crack propagation (uniaxial loading) we start with the pre-notched and thermalized slab and impose uniaxial expanding boundary conditions [1]. The cell length in the x direction $L_x(t)$ is continuously increased with time:

$$L_x(t) = L_x(0) + v_{\text{exp}}t = L_x(0) + L_{x0}\dot{\eta}t, \quad (1)$$

where $L_x(0)$ is the initial cell size in the x direction (2% strained), L_{x0} is the unstrained cell length, v_{exp} is the expansion velocity, and $\dot{\eta}$ is the strain rate. The cell parameter is increased at every time step during the MD simulation which leads to a continuous uniaxial expansion of the system.

Most of the atoms in the system are evolved using adiabatic MD during the expansion, the atoms with positions $0 < x < \delta$ and $L_x(t) - \delta < x < L_x(t)$ are thermalized in order to avoid overheating of the sample. We took $\delta = L_x(t)/10$; in this way around 20% of the atoms are thermalized. The thermalization is done by re-scaling the velocities of the atoms

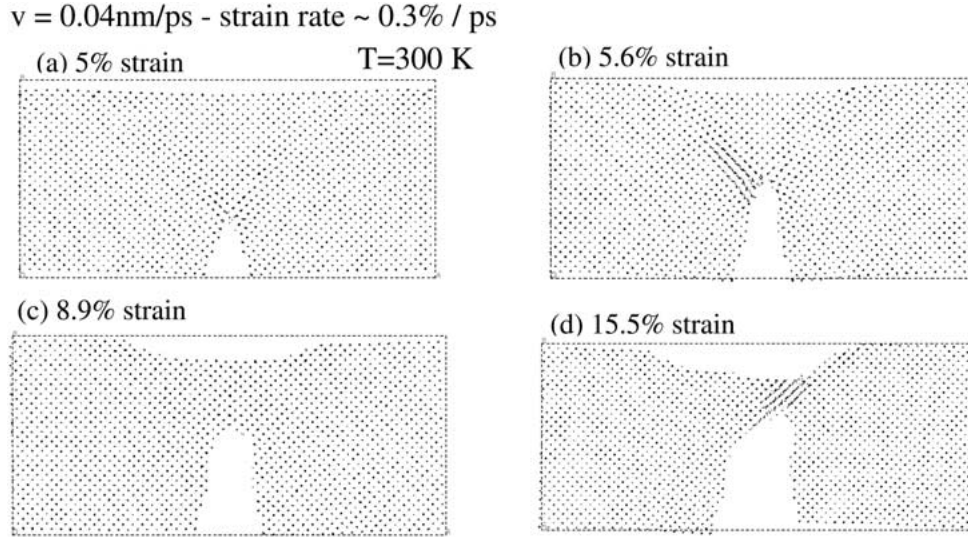


Figure 2. Snapshots of the system expanding with a velocity of $v_{\text{exp}} = 0.4 \text{ \AA/ps}$ at $T = 300 \text{ K}$. (a) 5% strain; (b) 5.6% strain, (c) 8.9% strain, and (d) 15.5% strain. At 5.6% strain the crack starts to emit dislocations; the dislocations then move towards the free surface and annihilate making steps on the surface (c).

once the local collective motion is taken into account. In practice the thermalization is done in the following way. We divide the system in $n = 10$ slices in the direction of the load. We define the collective velocity of region i (u_i) as:

$$u_i(t) = \frac{1}{N_i} \sum_j^{N_i} v_j(t), \quad (2)$$

where the sum runs over the N_i atoms (j) in region i and $v_j(t)$ is the velocity of atom j . The total kinetic energy of the slice i can be written as a sum of two terms: one related to the collective or center of mass motion and one involving velocity fluctuations around the mean collective velocity:

$$K_i = \frac{1}{2} M_i u_i^2 + \frac{1}{2} \sum_j^{N_i} m_j (v_j - u_i)^2, \quad (3)$$

where M_i is the total mass in region i and m_j is the mass of atom j . The local temperature is related to the internal kinetic energy. The local temperature of slice i is defined by:

$$K_i = \frac{1}{2} N_{df} k T_i, \quad (4)$$

where k is Boltzmann's constant, N_{df} is the number of degrees of freedom in region i and T_i is its local temperature. The number of degrees of freedom is $N_{df} = 3N_i - 3$ since the c.m. velocity of the system has been zeroed. Once the local temperatures are calculated the thermalization is accomplished by the following modification of the velocities:

$$v_j^{\text{new}} = (v_j^{\text{old}} - u_i) \sqrt{T/T_i} + u_i, \quad (5)$$

where T is the desired temperature. This procedure thermalizes the system without modifying the collective motion.

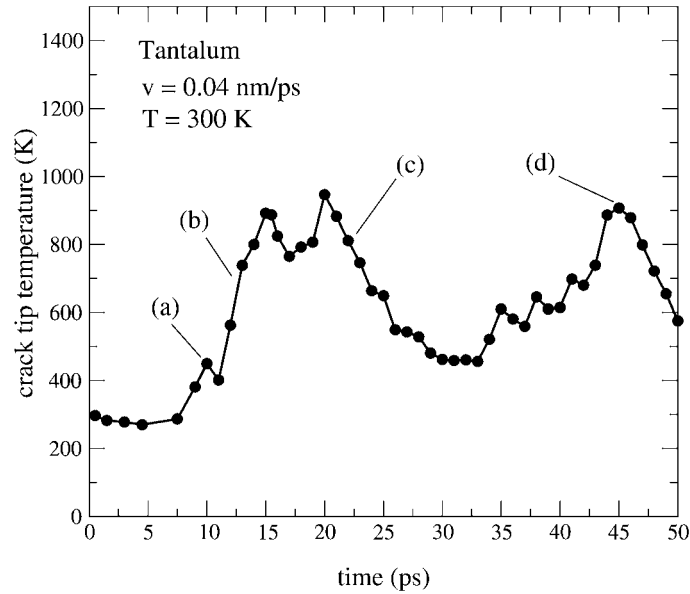


Figure 3. Local temperature of the crack tip for $v_{\text{exp}} = 0.4 \text{ \AA/ps}$ as a function of time. The marked points correspond to the panels in Fig. 2. The local temperature of the crack tip reaches high values during dislocation emission.

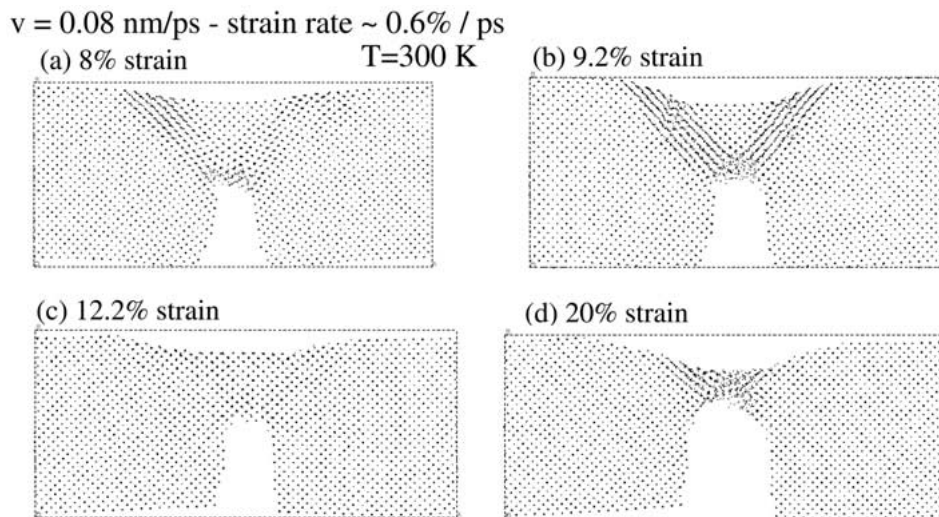


Figure 4. Snapshots of the system expanding with a velocity of $v_{\text{exp}} = 0.8 \text{ \AA/ps}$ at $T = 300 \text{ K}$. (a) 8% strain; (b) 9.2% strain, (c) 12.2% strain, and (d) 20% strain. Dislocations are emitted by the crack and later annihilated in the surface.

More sophisticated methods of thermalization, designed to damp the sound waves emitted by the crack motion and minimize the finite size effects, have been proposed, see for example [1].

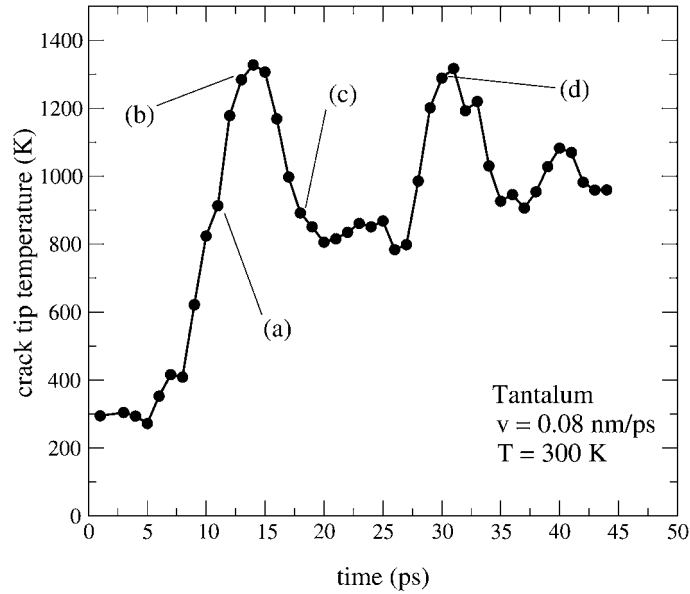


Figure 5. Local temperature of the crack tip for $v_{\text{exp}} = 0.8 \text{ \AA/ps}$ as a function of time. The marked points correspond to the panels in Fig. 2.

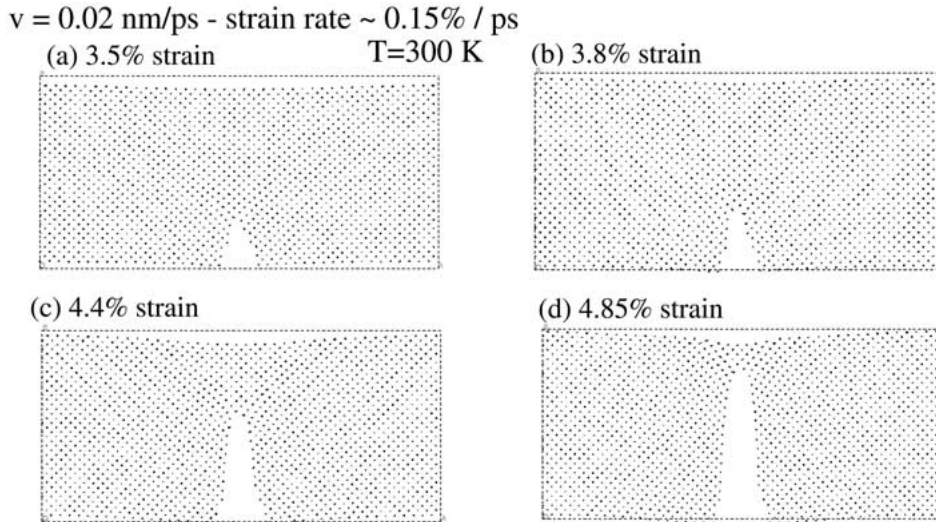


Figure 6. Snapshots of the system expanding with a velocity of $v_{\text{exp}} = 0.2 \text{ \AA/ps}$ at $T = 300 \text{ K}$. (a) 3.5% strain; (b) 3.8% strain, (c) 4.4% strain, and (d) 4.85% strain. The crack propagates in a brittle fashion, i.e. by bond breaking along a cleavage plane.

3. Strain rate and temperature effects on dislocation emission from the crack tip

We performed various simulations of crack propagation with expansion velocities in the range $0.1 \text{ \AA/ps} = 10 \text{ m/s} \leq v_{\text{exp}} \leq 1 \text{ \AA/ps} = 100 \text{ m/s}$, leading to strain rates in the range $0.075\% \text{ 1/s}$ to $0.75\% \text{ 1/s}$. The simulations were done at $T = 300 \text{ K}$ and $T = 600 \text{ K}$.

Fig. 2 shows the results of the MD simulations for $v_{\text{exp}} = 0.4 \text{ \AA/ps} = 40 \text{ m/s}$, $\epsilon \sim 0.3\%/ps$ at $T = 300 \text{ K}$; we show different snapshots of the system at different times. We find that the

crack starts to propagate in a brittle fashion, i.e. by bond breaking in a cleavage plane; Fig. 2a shows the configuration of the system at 5% strain ($t = 10$ ps) where we can see that the crack has advanced ~ 3 lattice parameters. At 5.6% strain we see, Fig. 2b, that a dislocation is being emitted from the crack tip. Several dislocations are emitted following this first one at 45 and -45 degrees from the propagation direction. The dislocations move towards the upper, free, surface and annihilate leaving steps on the surface, see Fig. 2c. At this point (8.9% strain) the system has relaxed back to its perfect bcc order. More dislocations are emitted at longer times to accommodate the deformation, Fig. 2d.

In order to gain a better understanding of the atomistic processes going on at the crack tip, we studied the time evolution of the local temperature of the crack tip. To calculate this local quantity we divide the system with a rectangular grid in the x and y directions. We divide the system in 10 regions along x and in 6 regions along y . For each region we calculate the local temperature as explained in the previous section [Eqs 3-4]. Fig. 3 shows the time evolution of the local temperature of the crack tip for $v_{\text{exp}} = 0.4 \text{ \AA/ps}$; the points marked (a), (b), (c), and (d) correspond to the panels in Fig. 2. We can see that the local temperature of the crack tip reaches very high values (~ 700 K) before emitting dislocations. The processes of dislocation emission, their motion towards the surface and annihilation occurs between points marked (b) and (c); throughout this period of time the crack tip temperature ranges from ~ 700 K to ~ 1000 K. The emission of dislocations generates the necessary plastic deformation (slip) to relax the system, consequently, the local temperature at the crack tip decreases.

Fig. 4 shows four snapshots of the process at a higher strain rate, $v_{\text{exp}} = 0.8 \text{ \AA/ps} = 80 \text{ m/s}$, $\epsilon \sim 0.6\%/ps$, also at $T = 300$ K. The behavior is very similar to the one described above for $v_{\text{exp}} = 0.4 \text{ \AA/ps}$. We can also see dislocation emission from the crack tip, their annihilation at the surface and the recovery of the perfect bcc structure. Fig. 5 shows the local temperature of the crack tip; again, very high temperatures are obtained at the crack tip during the dislocation emission.

From Figs. 2–5 we can see that the temperature of the crack tip remains rather constant until it starts to advance. During its initial brittle-like propagation energy builds up in the crack tip, until this energy is high enough to emit dislocations.

Fig. 6 shows snapshots for $v_{\text{exp}} = 0.2 \text{ \AA/ps} = 20 \text{ m/s}$ at 300 K; in this case the crack propagates throughout the slab without emitting dislocations. The full line in Fig. 7a shows the corresponding local temperature of the crack tip (for $v_{\text{exp}} = 20 \text{ m/s}$). At this lower velocity the crack reaches the free surface before accumulating the necessary energy to emit dislocations. Notice that at 4.85% strain the crack has almost reached the free surface and its local temperature is ~ 600 K. The dashed line in Fig. 7b shows the time evolution of the crack tip temperature for $v_{\text{exp}} = 0.1 \text{ \AA/ps} = 10 \text{ m/s}$ at 300 K; for this strain rate we also find that no dislocations are emitted. Fig. 7b shows the time evolution of the crack position for $v_{\text{exp}} = 0.2 \text{ \AA/ps}$ (full line) and $v_{\text{exp}} = 0.1 \text{ \AA/ps}$ (dashed line). It is very interesting to see that the crack moves in steps. The process consists of periods of time in which the crack advances fast (5 \AA/ps) leading to a large increase of the local temperature, followed by times of no advance of the crack at which the local temperature of the crack tip decreases.

From Figs. 3, 5 and 7a we expect dislocations to be emitted from the crack for the lower velocities ($v_{\text{exp}} = 0.1 \text{ \AA/ps}$ and $v_{\text{exp}} = 0.2 \text{ \AA/ps}$) had we used a thicker slab. Instead of a larger system we performed a simulation at a higher initial temperature ($T = 600$ K), for the same velocity $v_{\text{exp}} = 20 \text{ m/s}$. Fig. 8 shows different snapshots of the process at different times for $v_{\text{exp}} = 20 \text{ m/s}$ and $T = 600$ K; as expected at this higher temperature the crack emits

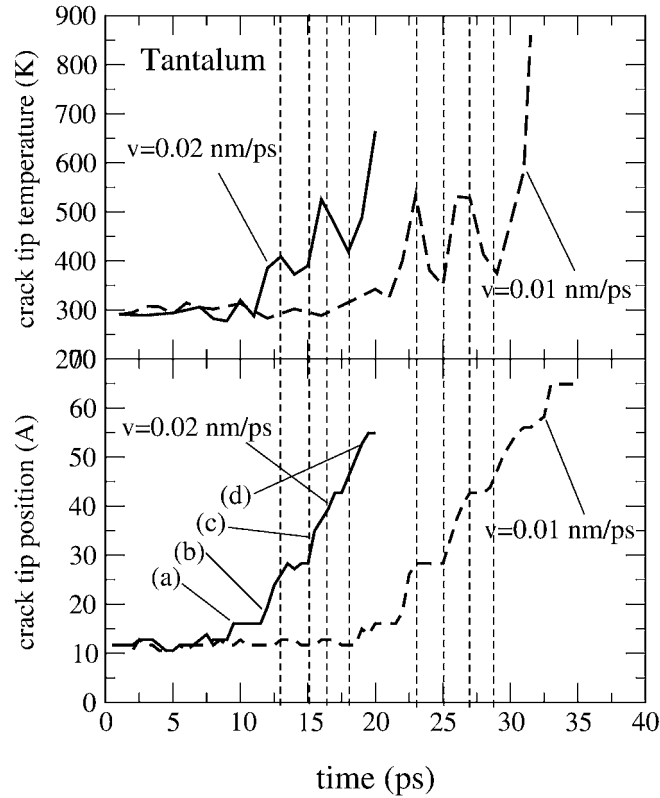


Figure 7. (a) Local temperature of the crack tip for $v_{\text{exp}} = 0.2 \text{ \AA/ps}$ (full line) and $v_{\text{exp}} = 0.1 \text{ \AA/ps}$ as a function of time, for $T = 300 \text{ K}$. (b) Position of the crack tip for $v_{\text{exp}} = 0.2 \text{ \AA/ps}$ (full line) and $v_{\text{exp}} = 0.1 \text{ \AA/ps}$ as a function of time. We can see that the crack moves in steps; while the crack moves the local temperature grows; this motion is followed by periods of time in which the crack stays motionless and the local temperature of the crack tip decreases.

dislocations. Fig. 9 shows the time evolution of the temperature of the crack tip; as in previous cases dislocations are emitted when the crack tip reached temperatures around 700 K.

4. Discussion

We studied via MD the process of crack propagation in a pre-notched Tantalum nano-slab under uniaxial deformation in a [100] direction. We studied a wide range of strain rates (0.075% 1/s to 0.75% 1/s) and temperatures $T = 300 \text{ K}$ and $T = 600 \text{ K}$.

In all our simulations we find that the crack starts to advance in a brittle fashion, i.e. by bond breaking in a cleavage plane. While the crack moves energy builds up in the crack tip, this leads to high values of the local temperature at the crack tip. This accumulation of energy at the crack tip leads, eventually, to the emission of dislocations; the plastic deformation relaxes the system causing a decrease of the local temperature. For our small slabs, we find that for expansion velocities of 0.1 \AA/ps and 0.2 \AA/ps the crack propagates through the whole sample without emitting dislocations; this is because not enough energy is concentrated in the crack tip. For the same expansion velocities, higher initial temperature (such as $T = 600 \text{ K}$)

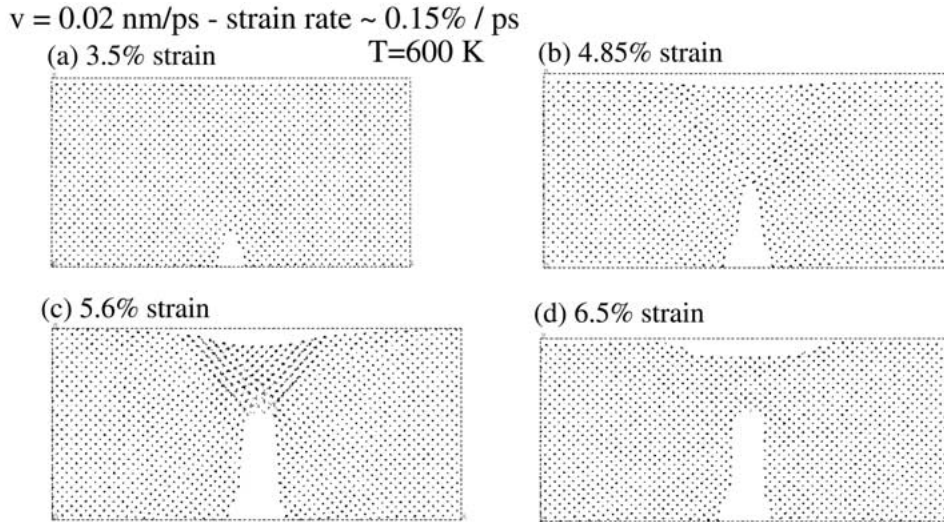


Figure 8. Snapshots of the system expanding with a velocity of $v_{\text{exp}} = 0.2 \text{ \AA/ps}$ at $T = 600 \text{ K}$. (a) 3.5% strain; (b) 4.85% strain, (c) 5.6% strain, and (d) 6.5% strain. At 5.6% strain the crack emit dislocations; the dislocations then move towards the free surface and annihilate making steps on the surface (c).

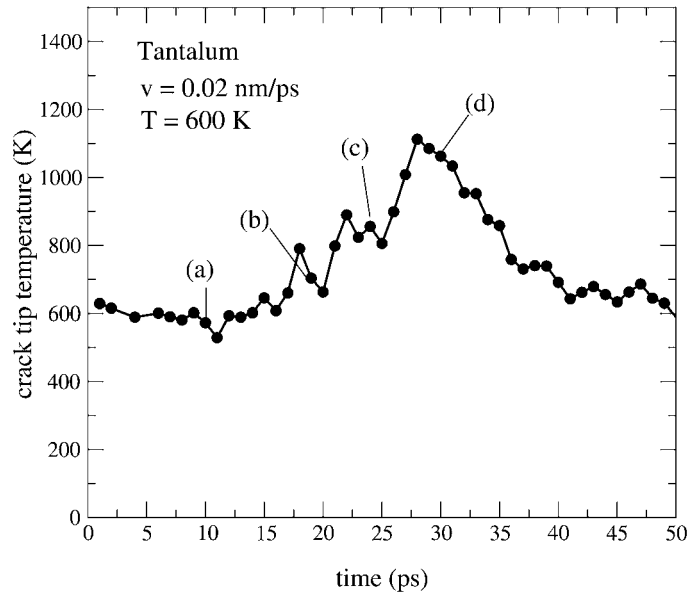


Figure 9.

leads to dislocation emission. We find that dislocations are emitted when the temperature of the crack tip is around 700 K.

We also find that during brittle propagation the cracks advance step wise. When the crack moves the temperature of its tip increases; then the crack stops propagating leading to a decrease of the local temperature. In order to have brittle propagation, low temperatures of the crack tip are needed.

Acknowledgements

This research was funded by a grant from DOE-ASCI-ASAP. The facilities of the MSC are also supported by grants from NSF (MRI CHE 99), ARO (MURI), ARO (DURIP), NASA, BP Amoco, Exxon, Dow Chemical, Seiko Epson, Avery Dennison, Chevron Corp., Asahi Chemical, 3M, and Beckman Institute.

References

1. Holian, B.L. and Ravelo, R., Phys. Rev. B 51 (1995) 11275.
2. Zhou, S.J., Lomdahl, P.S., Thomson, R. and Holian, B.L., Phys. Rev. Lett. 76 (1996) 2318.
3. Zhou, S.J., Beazley, D.M., Lomdahl, P.S. and Holian, B.L., Phys. Rev. Lett. 78 (1997) 479.
4. Gumbsh, P., Zhou, S.J. and Holian, B.L., Phys. Rev. B 55 (1997) 3445.
5. Cleri, F., Yip, S., Wolf, D. and Phillpot, S.R., Phys. Rev. Lett. 79 (1997) 1309.
6. Shiotz, J., Canel, L.M. and Carlsson, A.E., Phys. Rev. B 55 (1997) 6211.
7. Knap, J. and Sieradzki, K., Phys. Rev. Lett. 82 (1999) 1700.
8. Cheung, K.S. and Yip, S., Phys. Rev. Lett. 65 (1990) 2804.
9. Tang, Q. and Wang, T., Comp. Mat. Sci. 12 (1998) 73.
10. Holland, D. and Marder, M., Phys. Rev. Lett. 80 (1998) 746; Hauch, J.A., Holland, D., Marder, M. and Swinney, H.L., Phys. Rev. Lett. 82 (1999) 3823.
11. Miller, R., Ortiz, M., Phillips, R., Shenoy, V., Tadmor, E.B., Eng. Fract. Mech. 61 (1998) 427; Shenoy, V.B., Miller, R., Tadmor, E.B., Phillips, R. and Ortiz, M., Phys. Rev. Lett. 80 (1998) 742; Broughton, J.Q., Abraham, F.F., Bernstein, N. and Kaxiras, E., Phys. Rev. B 60 (1999) 2391.
12. Strachan, A., Çağın, T., Gülseren, O., Mukherjee, S., Cohen, R.E. and Goddard III, W.A., Phys. Rev. B (submitted).
13. Wang, G., Strachan, A., Çağın, T., Goddard III, W.A., Mat. Sci. Eng. A 309 (2001) 133.
14. Strachan, A., Çağın, T. and Goddard III, W.A., Phys. Rev. B63 (2001) 060103.